ARMA 20–1199

SAND2020-2631C

Enhancement mechanisms of induced seismicity by site-specific operational and geological features in a poroelasticity system

Chang, K.W.
Geotechnology & Engineering Department, Sandia National Laboratories, Albuquerque, NM, USA
Yoon, H.
Geomechanics Department, Sandia National Laboratories, Albuquerque, NM, USA
Kim, Y.-H.
School of Earth and Environmental Sciences, Seoul National University, Republic of Korea
Lee, M.Y.
Geomechanics Department, Sandia National Laboratories, Albuquerque, NM, USA

ABSTRACT: Recent occurrence of moderate to large seismic events (Mw ≥ 3) after terminating well operations is unlikely to be caused only by pore-pressure diffusion into conductive faults; it is necessary to address additional mechanisms in the earthquake nucleation. Our coupled fluid flow and geomechanical model describes the processes inducing seismicity corresponding to the sequential stimulation operations in Pohang, South Korea. Simulation results show that the combined effect of poroelastic shearing and delayed pore-pressure accumulation can cause slip on a fault, potentially inducing the post shut-in large earthquakes. Alternate injection-extraction operations through multiple wells can enhance the efficacy of pore-pressure diffusion and subsequent stress transfer through rigid and low-permeability basement rocks to the fault. This mechanistic study addresses that comprehensive characterization of the faulting system and optimal injection-extraction strategies are critical to mitigate unexpected seismic hazards associated with the site-specific uncertainty in operational and geological factors.

1. INTRODUCTION

Over the past decade a number of induced seismic events have been increasingly observed due to extensive subsurface energy activities such as wastewater injection [e.g., Kim, 2013, Hornbach et al., 2016], geothermal stimulation [e.g., Diehl et al., 2017], or geological carbon storage [e.g., Bauer et al., 2016]. Numerical models provide a critical link between field observations and theory of mechanisms inducing earthquakes by quantifying transient perturbations in pore pressure and stresses throughout a domain of interest.

At the Pohang site in South Korea (Fig. 1), the first EGS stimulation began on 29 January 2016 and total of five phases of injection-production operations had taken place at ~4.3 km of depth through PX-1 and PX-2 wells until September 2017 with a net injected volume of 6,000 m^3 (total injected volume of 12,800 m^3 and total produced volume of 6,800 m^3). The spatial footprint of detected seismic events delineates the geometry of the fault plane (strike/dip = N214°/43°NW), separating PX-1 and PX-2 [GSK2019], which was not found prior to the EGS stimulation. The focal mechanisms indicate that the Korean Peninsula is under tectonic compression, and the local stress field reveals that the 2017 Pohang earthquake was induced by the oblique reverse slip of a previously extensional fault at optimal orientation. This fault was critically stressed, implying that a fault slips with a small stress perturbation, and drilling or fluid injection-production initiated seismic activities along the fault.

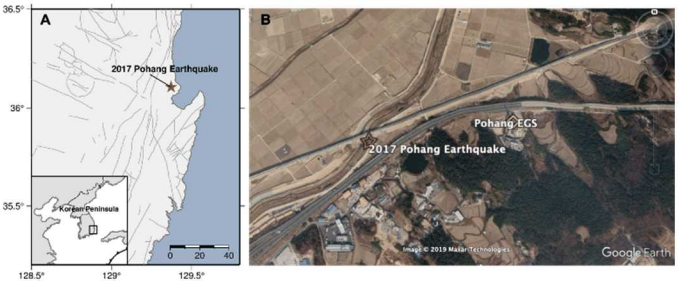

Fig. 1. Locations of the 2017 Mw5.5 Pohang earthquake and EGS site.

The lack of seismicity in the area prior to the EGS operation and the proximity of the 2017 Pohang earthquake to an EGS site strongly support the feasibility

Sandia National Laboratories is a multimission laboratory managed and operated by National Technology & Engineering Solutions of Sandia, LLC, a wholly owned subsidiary of Honeywell International Inc., for the U.S. Department of Energy's National Nuclear Security Administration under contract DE-NA0003525.

of labeling the Pohang earthquake a human-induced event [GSK, 2019].

Two critical questions about the 2017 Mw5.5 Pohang earthquake should be elaborated through theoretical and numerical approaches. First, why was the occurrence of the 2017 Pohang earthquake delayed two months after terminating stimulation? Site-specific characteristics of geological formation and/or operational constraints (e.g., injection-extraction rate and duration) affect the temporal pattern of induced seismicity as observed at other energy exploration sites [Keranen et al., 2014, Mukuhira et al., 2017], but still physics-based mechanisms for the occurrence of post shut-in seismic events have remained uncertain. Second, how could the Mw5.5 magnitude event be caused by human activity? The maximum magnitude of earthquake driven by subsurface energy exploration will be bounded by elastic strain energy and elevated pore pressure along the seismogenic fault plane. A theoretical scaling relation between the maximum earthquake magnitude and the total injected volume [McGarr, 2014] estimates three orders of magnitude more injected volume required to induce an earthquake of Mw5.5, which invalidates the use of this relation (Fig. 2).

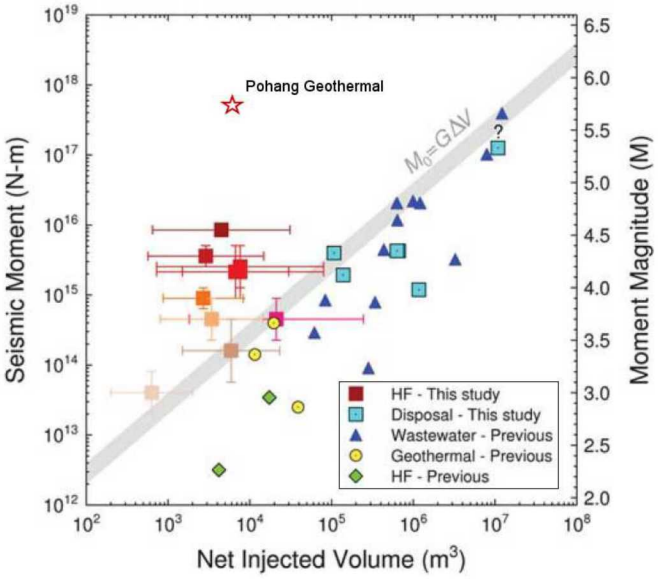

Fig. 2. Relationship between seismic moment and total injected fluid volume. The Pohang earthquake is way off the trend line estimated by McGarr [2014].

2. UNCOUPLED HYDROLOGICAL MODEL

Hydrological modeling approaches have focused on the direct pore-pressure impact on the fault slip and suggested the enlargement of pressurized regions encountering the locked fault as a key factor to induce earthquakes. The gradual accumulation of pore pressure within the permeable fault is essential to nucleate large-magnitude earthquakes after shut-in [e.g., Talwani and Acree, 1984].

A hydrological model tried to match stimulation history and the temporal evolution of seismic events observed at Pohang by setting the hydraulic diffusivity of the basement rock surrounding the fault plane to 1×10^{-2} m^2/s that was the practical upper limit of the hydraulic diffusivity (measured values within $1\times10^{-4} \le D_b \le 1\times10^{-2}$ m^2/s; refer to Fig. 6-1 and Section 6.2.1. in GSK [2019]). However, the Mw5.5 event is unlikely to occur due to substantial dissipation of elevated pore pressure into the high-diffusivity basement after extraction or shut-in (Fig. 2).

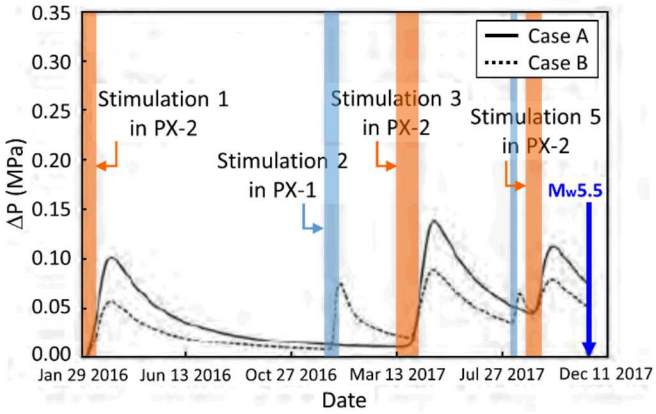

Fig. 3. The pore-pressure evolution corresponding to each stimulation phase at the hypocenter of Mw5.5 event from uncoupled hydrological modeling (modified Fig. O-15b in GSK [2019]).

3. COUPLED MODEL

The volumetric changes of the pressurized zone perturb the stress field of the surrounding rock that transmits forces to great distances even beyond the hydraulically affected region ("poroelastic stressing"), which has been addressed as an additional mechanism inducing earthquakes on basement faults. Recent coupled poroelastic studies revealed that indirect transmission of stresses can initiate seismic events along the fault, in particular, the increase of after shut-in events [e.g., Chang and Segall, 2016, Zhai et al., 2019].

Here we implemented poroelastic coupling in our model with $D_b = 1\times10^{-4}$ m^2/s that describes the role of poroelastic stressing caused by each stimulation phase in the earthquake occurrence as well as gradual accumulation of pore pressure within the fault zone. The fault is conductive but hydraulically isolated from the basement, and thus, the effects of direct pore-pressure diffusion and indirect stress transfer on the fault stability are primarily affected by the properties of the basement rock and/or the hydraulic connectivity through the conductive pathway [Chang and Yoon, 2018].

The poroelastic response to each stimulation phase at either side of the fault determines stress components in space acting on the fault plane, and thus, we first distinguished stimulation activities by PX-1 and PX-2 operations respectively, not merely by combined injection

and extraction volume changes as done in hydrological modeling approaches (Fig. 4A).

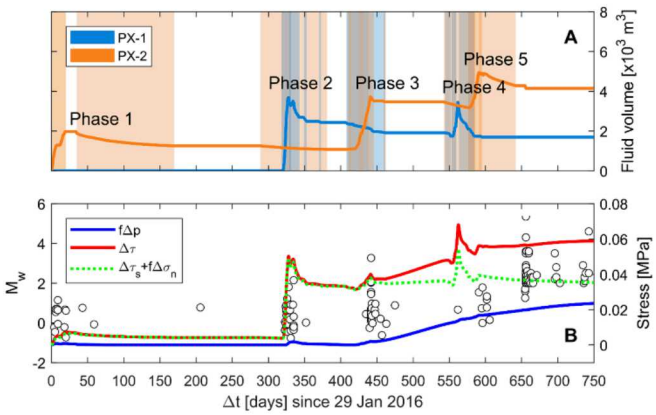

Fig. 4. A. Stimulation history categorized by PX-1 and PX-2 wells [GSK, 2019]. The accumulative injection volume for each well is indicated by blue and orange lines, respectively. B. The coupled fluid flow and geomechanical model produces poroelastic stressing ($\Delta\tau_s+f\Delta\sigma_n$) that captures the seismic events reasonably. Delayed pore-pressure accumulation results in larger $\Delta\tau$ even after stimulation wells have been shut-in.

The Coulomb stress change ($\Delta\tau$) from the initial stress state is used as a proxy for induced earthquakes on the critically-stressed faults. The effects of poroelastic stressing and pore-pressure diffusion on $\Delta\tau$ are evaluated using two terms: pore pressure change ($f\Delta p$) and the sum of the shear and normal stress components ($\Delta\tau_s+f\Delta\sigma_n$, where f is the fault friction coefficient). The uncoupled system used in conventional approaches perturbs pore-pressure fields only, such that $\Delta\tau = f\Delta p$.

The temporal evolutions of Coulomb stress components suggest that two physical processes control temporal sequences of seismic events along the permeable fault (Fig. 4B). Rapid poroelastic response to stimulation phases generates immediate increases in $\Delta\tau_s+f\Delta\sigma_n$ that contribute to induced seismic events during and after Phases 2 and 3 even without direct pore-pressure effects. Once pore pressure diffuses into the fault, gradual increases in $f\Delta p$ reduce the normal load acting on the fault plane, which leads to larger $\Delta\tau$, thereby causing more substantial aftershocks. Note that the presence of high-permeability structures, e.g., fractures, or larger injection rates and longer stimulation periods will enhance the stress transmission and pore-pressure diffusion to the fault, ultimately raising $\Delta\tau$ along the fault.

We further analyzed the spatial patterns of seismic events that were fitted to the distribution of $\Delta\tau$ along the middle of the fault plane over time (the fault top and bottom are located at depth of -3.6 and -4.6 km, respectively; Fig. 5). Considering the vertical distribution of pore-pressure and stress fields along the fault, the poroelasticity model generates depth-dependent changes in $\Delta\tau$ corresponding to the stimulation activities and well locations (Fig.5).

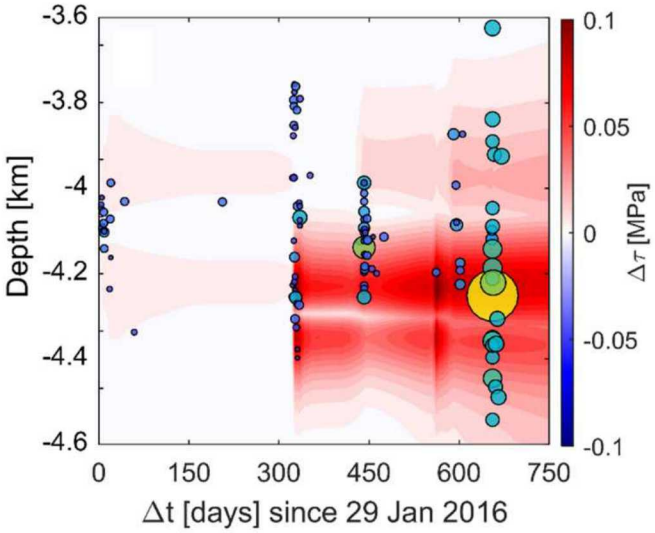

Fig. 5. The distribution of $\Delta\tau$ along the middle of the fault zone and the seismic events over time. The magnitude of earthquakes varies with size and color of circles. The coupled model fits earthquakes to $\Delta\tau$ in space and time, and the incorporated effect of poroelastic stressing and pore-pressure accumulation can generate the Mw5.5 event after terminating stimulation activities.

Before undergoing direct pore-pressure effects, shear stressing on the fault plane induces instantaneous seismic events as poroelastic response to the simulation Phases 1 to 3. Note that some seismic activities (especially, ones at the depth of ~3.8 km after Phase 2 stimulation; $\Delta t \approx$ 335 days) distribute off the area of positive changes in $\Delta\tau$, which indicates that these earthquakes were induced by hydraulic fracturing or reopening preexisting fractures away from the seismogenic fault plane. After pore pressure diffuses into the fault zone ($\Delta t \geq 450$ days), either instantaneous poroelastic stressing or increase in pore pressure (or both) provides an adequate mechanism for weakening the fault plane. The prolonged diffusion of pore pressure generates a broader distribution of seismic events along the fault. Accumulation of poroelastic strain energy and pore pressure directly diffused from both sides of the fault can be sufficient to generate a large-magnitude earthquake along the fault, which explains the Mw5.5 earthquake observed at the depth of ~4.27 km after shut-in GSK [2019]. The spatio-temporal matches between $\Delta\tau$ and a series of seismic events validates our poroelasticity model, which emphasizes the importance of applying multiphysics system for the numerical approach to define physical mechanisms for induced earthquakes.

4. OPERATIONAL CONSTRAINTS

A better understanding of the driving mechanisms underlying the Pohang earthquake occurrence requires a

reexamination of the operational controls on induced seismicity. A simultaneous or sequential operation of injection-extraction has been proposed as a mitigation strategy to minimize geomechanical failure of the target formation by maintaining pore-pressure fields below the threshold for fault slip based on a mass balance approach [Dempsey et al., 2014, Scanlon et al., 2018]. Both the number of wells and the well locations with respect to the fault plane are the most essential parameters controlling earthquakes to limit the seismic hazards posed by given injection-production scenarios.

Here we conducted a coupled simulation with a single-well operation in which whole injection-extraction activities were operated only through PX-2. Note that a single-well operation setting only aims to look into how operational constraints influence the mechanical stability of preexisting weak structures, not considering the efficacy of well design for a heat exchanger.

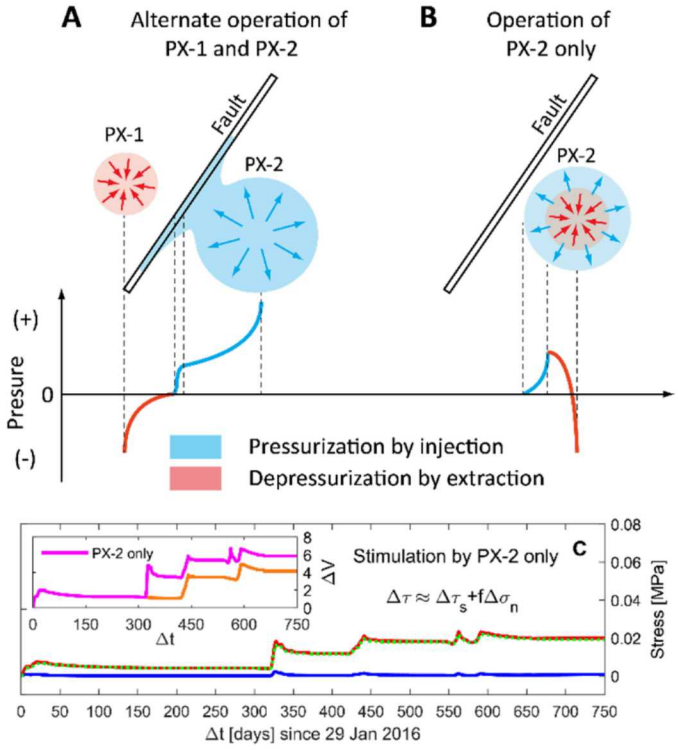

Fig. 6. A. Alternate injection-extraction through PX-1 and PX-2 causes stronger gradients in pore-pressure fields across the fault that enhances the efficiency of pore-pressure diffusion into the fault. B. Repeated injection-extraction through PX-2 only limits the extent of pressurization that eliminates direct pore-pressure effects on fault slip. C. The single-well model in which the whole stimulation activities are conducted only through PX-2 gives no substantial pore-pressure buildup, such that $\Delta\tau \approx \Delta\tau_s + f\Delta\sigma_n$. The alternate injection-extraction through PX-1 and PX-2 develops stronger gradients in pore-pressure field across the fault that enhance the efficiency of diffusion into the fault. The cyclic injection-extraction only through PX-2 limits the extent of pressurization even though larger accumulative volume is achieved.

A single-well stimulation causes larger accumulation of net injected volume nearby PX-2 (indicated by a magenta line in inset plot of Fig. 6C), which may lead to substantial enlargement of the pressurized region around PX-2.

However, the cyclic injection-extraction at a single well limits the extent of pressurized region that prevents direct pore-pressure effects on the fault, such that no substantial elevation of pore pressure is observed over time ($\Delta\tau \approx \Delta\tau_s + f\Delta\sigma_n$; Fig. 6C). On the other hand, alternate injection-extraction through PX-1 and PX-2 prompts strong gradients in pore-pressure fields across the fault plane that magnify the efficiency of transmitting fluid pressure and stresses through low-permeability basement rocks. This mechanism causes incorporated effects of poroelastic stressing and pressure buildup after stimulation Phase 3 ($\Delta t \geq 450$ days).

This result emphasizes the need for proper well design and operating strategy with respect to the geometry of preexisting faults to avoid unexpected perturbations in stress states. Installing multiple wells parallel to realized preexisting faults will minimize potential pore-pressure diffusion and corresponding stress transfer to the faults. Gradual retardation of injection-extraction rates can mitigate gradients in pore-pressure fields across the fault.

5. CONCLUSIONS

The key finding of this study is that the sequential processes of poroelastic shearing and/or pore-pressure diffusion control spatio-temporal distributions of seismic events at the Pohang EGS site, given geological and operational characteristics [GSK, 2019]. Poroelastic stressing can promote the activation of distant, large faults that are close to failure without requiring a direct hydraulic connection. The poroelastic coupling scheme overcomes the limit of conventional approaches using hydrological models that constrain the direct effect of pore-pressure accumulation as an exclusive mechanism inducing seismicity, and should be included in the assessment of seismic hazards associated with fluid injection-extraction.

The Mw5.5 event after shut-in is achievable if delayed pore-pressure accumulation and poroelastic shearing brought about failure of the fault. Strong pressure gradients driven by sequential stimulation through PX-1 and PX-2 enabled pore-pressure accumulation within the fault, which is an additional mechanism responsible for the extensive seismogenic response to the ESG stimulation activities. Therefore, comprehensive formation characterization and optimal injection-extraction strategies are critical to mitigating potential seismic hazards associated with massive injection of fluids.

ACKNOWLEDGEMENTS

K.W.C., M.Y.L. and H.Y. are supported by the Laboratory Directed Research and Development program at Sandia National Laboratories. Y.K. acknowledges support from the Creative Pioneering Researchers Program of Seoul National University (SNU SRnD 3345-20160014). Sandia National Laboratories is a multimission laboratory managed and operated by National Technology and Engineering Solutions of Sandia, LLC., a wholly owned subsidiary of Honeywell International, Inc., for the U.S. Department of Energy National Nuclear Security Administration under contract DE-NA-0003525. This paper describes objective technical results and analysis. Any subjective views or opinions that might be expressed in the paper do not necessarily represent the views of the U.S. Department of Energy or the United States Government.

REFERENCES

1. Bauer, R.A. M. Carney, and R.J. Finley (2016), Overview of microseismic response to CO2 injection into the Mt. Simon saline reservoir at the Illinois Basin-Decatur Project, *Int. J. Green. Gas Con.*, 54(1):378-388.
2. Chang, K.W. and P. Segall (2016), Injection induced seismicity on basement faults including poroelastic stressing, *J. Geophys. Res. Solid Earth*, 121(4):2708-2726.
3. Chang, K.W. and H. Yoon (2018), 3-D modeling of induced seismicity along multiple faults: Magnitude, rate, and location in a poroelasticity system, *J. Geophys. Res. Solid Earth*, 123(11):9866-9883.
4. Dempsey, D., S. Kelkar, and R. Pawar (2014), Passive injection: A strategy for mitigating reservoir pressurization, induced seismicity and brine migration in geologic CO_2 storage, *Int. J. Greenh. Gas Con.*, 28:96-113.
5. Diehl, T. , T. Kraft, E. Kissling, and S. Wiemer (2017), The induced earthquake sequence related to the St. Gallen deep geothermal project (Switzerland): Fault reactivation and fluid interactions imaged by microseismicity, *J. Geophys. Res. Solid Earth*, 122(9):7272-7290.
6. Geological Society of Korea (GSK) (2019), Summary report of the Korean Government Commission on relations between the 2017 Pohang earthquake and EGS project.
7. Keranen, K.M., M. Weingarten, G.A. Abers, B.A. Bekins, and S. Ge (2014), Sharp increase in central Oklahoma seismicity since 2008 induced by massive wastewater injection, *Science*, 345:448.
8. Kim, W. Y. (2013), Induced seismicity associated with fluid injection into a deep well in Youngstown, Ohio, *J. Geophys. Res. Solid Earth*, 118(7):3506-3518.
9. McGarr, A. (2014), Maximum magnitude earthquakes induced by fluid injection, *J. Geophys. Res. Solid Earth*, 119(2):1008-1019.
10. Mukuhira, Y., C. Dinske, H. Asanuma, T. Ito, and M. Haring (2017), Pore pressure behavior at the shut□in phase and causality of large induced seismicity at Basel, Switzerland, *J. Geophys. Res. Solid Earth*, 122(1):411-435.
11. Scanlon, B.R., M.B. Weingarten, K.E. Murray, and R.C. Reedy (2018), Managing Basin□Scale Fluid Budgets to Reduce Injection□Induced Seismicity from the Recent U.S. Shale Oil Revolution, *Seismol. Res. Lett.*, 90(1):171-182.
12. Talwani, P. and S. Acree (1984), Pore pressure diffusion and the mechanism of reservoir-induced seismicity, *Pure Appl. Geophys.,* 122(6):947-965.
13. Zhai, G., M. Shirzaei, M. Manga, and X. Chen (2019), Pore-pressure diffusion, enhanced by poroelastic stresses, controls induced seismicity in Oklahoma, *PNAS*, 116(33):16228-16233.